

に証明した。Keap1 による Nrf2 の機能抑制の解除が、生体防御酵素群の誘導の上で鍵となるステップであり、その分子メカニズムを解明する目的で以下の実験を行った。

B. 研究方法

(1) Nrf2 による転写活性化機構の解析

クロマチンリモデリング因子が、Nrf2 の転写活性化に必要であるという仮説を立てて、BAF 複合体に含まれる Brg1 の欠損細胞株における Nrf2 による転写活性化能を検討した。また、Brg1 と Nrf2 の転写活性化ドメインとの相互作用を検討した。さらに、野生型細胞において、Brg1 をその siRNA によりノックダウンした場合に、Nrf2 による転写活性化反応が抑制されるかどうかを検討した。また、Brg1 過剰発現細胞を樹立して、Nrf2 による転写活性化反応が亢進するかどうかを検討した。GST-Nrf2 融合タンパク質も作製し、Hela 細胞から調整した核抽出液を反応させて、Nrf2 に相互作用する核内蛋白質複合体を精製し、そこに含まれる因子を質量分析により同定した。

(2) Keap1 による刺激の感知機構の解析

親電子性物質、あるいは、活性酸素種などの刺激に対する反応性の実体は Keap1 による Nrf2 の抑制の解除である。このことから、Keap1 による Nrf2 抑制のメカニズムと Keap1 による Nrf2 抑制解除のメカニズムを明らかにすることの必要性が理解される。本研究では、主に前者について解析を行った。まず、BTB、IVR、DGR の3つのドメインに大別される Keap1 の構造のうち、DGR ドメインの結晶構造を決定した。DGR ドメインは Nrf2 が結合する領域であり、Keap1 による Nrf2 の抑制に重要である。また、Keap1 により Nrf2 のプロテアソーム依存的な分解が促進されることを示し、Keap1 が Nrf2 のユビキチン化を促進するかどうかを検討した。さらに、Keap1 がユビキチンライゲース (E3) のアダプター分子として機能し、Nrf2 の分解に関与している可能性を考えて、Cullin ファミリー分子と Keap1 との結合を調べた。

C. 研究結果

(1) Nrf2 による転写活性化機構の解析

Brg1 欠損細胞株においては、野生型細胞株に比べて、Nrf2 による転写活性化の抑制が観察され、また、Brg1 は Nrf2 の転写活性化ドメインに直接相互作用することが示された。さらに、Brg1 ノックダウン細胞及び Brg1 過剰発現細胞をそれぞれ樹立し、Nrf2 活性化の指標として、Nrf2 の標的遺伝子である NQO-1 と HO-1 の発現レベルを調べた。その結果、Brg1 ノックダウン細胞では、HO-1 の転写活性化が障害されており、Brg1 過剰発現細胞では、HO-1 の転写活性化が亢進していた。しかしながら、NQO-1 の転写に対しては、両細胞とも対照細胞との間で差が認められず、Brg1 の重要性は標的遺伝子ごとに異なる可能性が示唆された。一方、Hela 細胞の核抽出液中から得られた Nrf2 に結合する蛋白質複合体に含まれる因子を、質量分析により同定したところ、クロマチンリモデリング因子やメディエーターとして TIF1 β が得られた。予備的ではあるが、TIF1 β が Nrf2 の転写活性化を促進するというレポーターアッセイの結果が得られている。

(2) Keap1 による刺激の感知機構の解析

Keap1 の DGR ドメインの結晶構造を決定したところ、通常の 6 角柱である β バレル構造とは異なり、6 つの側面構造のうち、1 番目の側面と 6 番目の側面が、咬み合わされる構造をとっていることが明らかになった。また、Nrf2 はバレルの底面に結合することが、同部位の Keap1 変異分子の検討から示唆された。一方、Nrf2 の N 末端領域が Keap1 依存的にユビキチン化されることが示され、また、Keap1 はユビキチンライゲースである Cullin3 と特異的に結合することが示された。すなわち、Keap1 はユビキチンライゲース Cullin3 のアダプター分子として機能することが明らかになった。さらに、定常状態における Cullin3-Keap1 による Nrf2 の分解には、Keap1 分子

の IVR ドメインに存在する 2 つのシステイン残基が必須であることが、レポーターアッセイなどの結果から明らかになった。

D. 考察

(1) Nrf2 による転写活性化機構の解析

Nrf2 は強力な転写活性可能を有しており、その分子基盤の解明は転写制御機構の解明という観点から非常に興味深い課題である。本研究から、Nrf2 の周辺で機能する因子群が明らかにされてきており、それらの貢献度が標的遺伝子の制御領域の環境によりどのように異なるのかを今後さらに明らかにしていく必要があると考えられる。

(2) Keap1 による刺激の感知機構の解析

Keap1 による Nrf2 の分解機構の解明は、本研究により大きく進展した。親電子性物質、あるいは、活性酸素種に曝露された場合には Nrf2 が核内に蓄積するが、その際に Nrf2 がどのようにして Keap1 による分解を免れるようになるのかは、まだ明らかではない。これらの刺激に応じて Cullin3-Keap1 を中心とするユビキチンライゲース活性が制御されるのか、あるいは、Nrf2 とユビキチンライゲース複合体との相互関係に変化が生じるのか、今後の検討課題である。

E. 結論

Nrf2-Keap1 制御系の分子機構を解析して、Nrf2 の転写活性化のメカニズムを担う因子群を同定し、Keap1 の Nrf2 機能抑制メカニズムを明らかにした。

F. 健康危険情報

特になし。

G. 研究発表

1. 薬剤の毒性発症における Nrf2-Keap1 制御系の重要性の検討 の項に同じ。

H. 知的財産権の出願・登録状況（予定を含む。）

特になし。

4. マウス個体における Nrf2 活性化分子機構の解析

研究要旨

Nrf2-Keap1 制御系の分子メカニズムは、前項の研究により、生化学的アプローチ、構造生物学的アプローチ、細胞生物学的アプローチにより詳細に検討された。しかしながら、Nrf2 と Keap1 の存在比により実験結果が大きく異なる場合があり、また、これらの *in vitro* システムでは、空気中の 20%酸素濃度のもとでの実験を余儀なくされるので、実際の生体内に比べてかなり酸化的環境での現象を検出していることになる。そこで、これらの問題点を解決するために、マウス個体レベルでの検証系として、重複ノックアウトレスキュー法とトランスジェニック相補レスキュー法を確立した。前者を用いた解析により、Nrf2 による転写活性化に必要な因子として、小 Maf 群因子を同定した。また、後者を用いた解析から、Keap1 の IVR ドメインに存在する 2 つのシステイン残基が実際に生体においても Keap1 の Nrf2 抑制機能に必須であることを証明した。さらに、培養細胞を用いたレポーターアッセイでは検出できなかった BTB ドメインの重要性を、マウス個体で試すことにより始めて示すことができ、同領域が Keap1 の Nrf2 抑制能に必須であることが明らかになった。

A. 研究目的

Nrf2-Keap1 制御系の分子メカニズムは、前項の研究により、生化学的アプローチ、構造生物学的アプローチ、細胞生物学的アプローチにより詳細に検討された。しかしながら、培養細胞を用いたレポーターアッセイでは、Nrf2 と Keap1 の存在比により実験結果が大きく異なる場合があり、また、これらのシステムでは、空気中の 20%酸素濃度のもとでの実験を余儀なくされるので、実際の生体内に比べてかなり酸化環境での現象を検出していることになる。特に、培養細胞は絶えず高酸素の環境にさらされており、Nrf2-Keap1 制御系が活性化されやすい状況におかれている。そこで、本研

究では、なるべく生理的条件に近い状況で、Nrf2-Keap1 制御系の機能解析をすることを目標とした。そのための手段として、マウス個体を用いた実験系を確立することにした。

B. 研究方法

(1) 検証系その1 (重複ノックアウトレスキュー法)

keap1 欠損マウスは、離乳期までに上部消化管における異常な角化亢進による摂食障害をきたして死亡するが、この表現型は、*keap1* と *nrf2* の2重欠損マウスを作成して、Keap1 と同時に Nrf2 も欠損させることにより完全に回復することから、*keap1* 欠損マウスの摂食障害による致死性は、恒常的に活性化された Nrf2 に依存している。したがって、ある因子の遺伝子欠損マウスを *keap1* 遺伝子欠損マウスと交配し、*keap1* 遺伝子欠損マウスの致死性が回避されるならば、その因子は Nrf2 の活性化に必要な因子であるといえる。この手法を用いて、小 Maf 群因子、あるいは、Ask1 の Nrf2 による転写活性化に対する重要性を検討した。具体的には、小 Maf 群因子欠損マウス、あるいは、*ask1* 遺伝子欠損マウスと *keap1* 遺伝子欠損マウスを交配して複合変異マウスを作成し、それらの寿命と体重増加、上部消化管の組織像、Nrf2 の標的遺伝子の発現レベルを調べた。

(2) 検証系その2 (トランスジェニック相補レスキュー法)

keap1 遺伝子の転写開始点上流 5.7 kbp の領域は、内在性の *keap1* 遺伝子の発現をほぼ再現できるということを LacZ 遺伝子をレポーターとしたブルーマウスアッセイにより明らかにした。そこで、同領域に Keap1 cDNA を結合してマウス受精卵に導入し、トランスジェニックマウスを作成した。本マウスは *keap1* 欠損マウスと交配すると、*keap1* 欠損による致死性をレスキューできた。そこで、Keap1 変異分子を *keap1* 遺伝子制御下に発現するトランスジェニックマウスを作成し、同マウスが *keap1* 欠

損マウスのレスキューをするかどうかを調べて、それら変異分子の機能検証を行った。

(3) 倫理面への配慮

本研究では遺伝子組換えマウスを実験に使用したが、その飼育、薬剤投与、屠殺にあたっては、動物愛護の精神にのっとり、与える苦痛が最小限になるように配慮した。また、無駄な屠殺を行うことがないように、計画を十分に吟味してから実験を行うようにつとめた。本実験計画は、すでに筑波大学動物実験委員会及び遺伝子組換え安全委員会に申請をおこない、それぞれから承認されている。

C. 研究結果

(1) 検証系その1 (重複ノックアウトレスキュー法)

小 Maf 群因子欠損マウスと *keap1* 遺伝子欠損マウスの交配により得られた複合変異マウスでは、致死性は回避され、生後4ヶ月以上生存可能であった。複合変異マウスの生後10日齢における前胃の組織像は、ほぼ正常であり Nrf2 の標的遺伝子として *keratin6* 遺伝子の発現レベルを調べたところ、*keap1* 欠損マウスでは著明に発現が亢進していたのに対して、複合変異マウスでは野生型マウスと同程度の発現レベルであった。しかしながら、週齢を重ねるにつれて、体重は野生型対照マウスに比べて少なくなり、上部消化管の組織像も、異常な角化亢進が認められるようになっていた。次いで、*ask1* 遺伝子欠損マウスと *keap1* 遺伝子欠損マウスを交配して複合変異マウスを得たが、こちらは、致死性を回避することはできず、*keap1* 遺伝子欠損マウスと同様に離乳期前後で死亡した。前胃の組織像、遺伝子発現とも、*keap1* 欠損マウスと複合変異マウスとの間に差異は認められなかった。

(2) 検証系その2 (トランスジェニック相補レスキュー法)

keap1 遺伝子の転写開始点上流 5.7 kbp の領域を LacZ 遺伝子に連結し、マウス受精

卵に導入してトランスジェニックマウスを作成したところ、得られた5ライン中4ラインで、内在性の *keap1* 遺伝子発現をほぼ再現することが可能であった。したがって、*keap1* 遺伝子の転写開始点上流 5.7 kbp の領域 (KRD5.7) には、内在性の *keap1* 遺伝子の発現をほぼ再現するのに十分な制御領域が含まれているものと判断した。そこで、同領域に Keap1 cDNA を結合させ、マウス受精卵に導入してトランスジェニックマウスを作成し、同マウスを *keap1* 欠損マウスと交配して複合変異マウスを作成した。この複合変異マウスは、野生型マウスと同様に生存可能であり、すなわち、トランスジェン由来の Keap1 が *keap1* 欠損による致死性をレスキューした。ここにトランスジェニック相補レスキュー法が確立できた。このシステムを利用して、Keap1 変異分子を *keap1* 遺伝子の制御下に発現するトランスジェニックマウスを作成し、同マウスが *keap1* 欠損マウスのレスキューをかけられるかどうかを調べることにより、それら変異分子の機能検証を行った。具体的には、これまで培養細胞を用いた実験から重要性が示唆されていた Keap1 IVR ドメインのシステイン残基の変異分子 (Keap1 CA mutant) と、これまで培養細胞を用いた実験では重要性が確認できていなかった BTB ドメインの欠失変異分子 (Keap1 Δ BTB) をそれぞれ KRD5.7 に連結して、トランスジェニックマウスを作成し、トランスジーンが発現量を確認のうえ、*keap1* 遺伝子欠損マウスと交配して、複合変異マウスを作成した。得られたマウスについて、寿命、体重、前胃の組織像と遺伝子発現をパラメーターとして、それぞれの Keap1 変異分子の機能を検討した。その結果、Keap1 CA mutant を発現する複合変異マウスも、Keap1 Δ BTB を発現する複合変異マウスもいずれも *keap1* 遺伝子欠損マウスと同様に離乳期で致死であった。前胃の異常な角化の亢進、Nrf2 標的遺伝子の発現亢進が認められた。これは、Keap1 IVR ドメインのシステイン残基と BTB ドメインが、いずれも定常状態における Keap1 による Nrf2 機能の抑制に必須であることを証明するものである。

D. 考察

(1) 検証系その1 (重複ノックアウトレスキュー法)

本研究の結果より、Nrf2 の転写活性化機能には小 Maf 群因子が必要であることが証明された。しかしながら、週齢を経るうちに、*keap1* 欠損マウスの表現型が顕在化してきたことから、小 Maf 群因子欠失による効果は、部分的であったと解釈できる。すなわち、Nrf2 の転写活性化には、小 Maf 群因子を必ずしも必要としない局面が存在する可能性が示唆される。一方、*ask1* 遺伝子欠損マウスとの交配は *keap1* 欠損マウスの致死性の回避にはいたらなかった。このことから、Nrf2 の転写活性化能には *ask1* の機能は必須ではない、もしくは、代償する分子が存在すると解釈できる。ストレス応答時に Ask1 が CBP をリン酸化することが報告されているが、CBP は Nrf2 の転写共役因子として機能することが示されている。このことから、Nrf2 の転写活性化には Ask1 による CBP のリン酸化が必要なのではないかと考えて実験を行ったが、この実験ではその仮説を実証することはできなかった。

(2) 検証系その2 (トランスジェニック相補レスキュー法)

生体内における生理的な酸化還元状態で、本来の Nrf2 と Keap1 の存在量に近い状況で Keap1 の分子機能の評価をすることが出来るシステムの構築に成功した。これにより、これまでの研究からその重要性が示唆されていた Keap1 IVR の2つのシステイン残基が、やはり生体内においても重要であることが確認された。さらに、このシステムの有効性を示す結果となったのは、培養細胞においては重要性がはっきりしていなかった Keap1 BTB ドメインが、Keap1 の機能に必須であることを明らかにできた点である。BTB ドメインは、Keap1 の2量体化をもたらすことが示されており、今後、Keap1 の2量体化がその機能にどのような意味をもつのかを検討する必要があると考えられる。

E. 結論

マウス個体を用いた Nrf2-Keap1 制御系の機能検証システムを確立し、同システムを用いることにより、生理的条件において、Nrf2 の転写活性化に小 Maf 群因子が必要であること、Keap1 IVR のシステイン残基と BTB ドメインがそれぞれ、Nrf2 機能の抑制のために必須であることが、明らかになった。

F. 健康危険情報

特になし。

G. 研究発表

1. 薬剤の毒性発症における Nrf2-Keap1 制御系の重要性の検討 の項に同じ。

H. 知的財産権の出願・登録状況（予定を含む。）

1. 特許取得

2004（平成 16）年度

特願 2004-319143 生体分子の相互作用観察方法（山本雅之，本橋ほづみ，京基樹，川上文清，稲森和紀）

特願 2004-319144 生体分子アレイ（山本雅之，本橋ほづみ，京基樹，川上文清，稲森和紀）

2. 実用新案登録

特になし

3. その他

特になし

研究成果の刊行に関する一覧表

発表者氏名	論文タイトル名	発表誌名	巻号	ページ	出版年
Itoh, K., Mochizuki, M., Ishii, Y., Ishii, T., Shibata, T., Kawamoto, Y., Kelly, V., Sekizawa, K., Uchida, K. and Yamamoto, M.	Transcription factor Nrf2 regulates inflammation by mediating the effect of 15-deoxy- $\Delta^{12,14}$ -prostaglandin J ₂ .	<i>Mol. Cell. Biol.</i>	24	36-45	2004
Kyo, M., Yamamoto, T., Motohashi, H., Kamiya, T., Kuroita, T., Tanaka, T., Kawakami, B. and Yamamoto, M.	Evaluation of MafG interaction with Maf recognition element arrays by surface plasmon resonance imaging technique.	<i>Genes Cells</i>	9	153-164	2004
Ishii, T., Itoh, K., Ruiz, E., Leake, D.S., Unoki, H., Yamamoto, M. and Mann, G.E.	Role of Nrf2 in the regulation of CD36 and stress protein expression in murine macrophages: activation by oxidatively modified LDL and 4-hydroxynonenal.	<i>Circulation Res.</i>	94	609-616	2004
Wakabayashi, N., Dinkova-Kostova, A.T., Holtzclaw, W.D., Kang, M.-I., Kobayashi, A., Yamamoto, M. , Kensler, T.W. and Talalay, P.	Protection against electrophile and oxidant stress by induction of the phase 2 response: Fate of cysteines of the Keap1 sensor modified by inducers.	<i>Proc. Natl. Acad. Sci. USA</i>	101	2040-2045	2004
Kang, M.I., Kobayashi, A., Wakabayashi, N., Kim, S.G. and Yamamoto, M.	Scaffolding of Keap1 to the actin cytoskeleton controls the function of Nrf2 as key regulator of cytoprotective phase 2 genes.	<i>Proc. Natl. Acad. Sci. USA</i>	101	2046-2051	2004
Motohashi, H., Katsuoka, F., Engel, J.D. and Yamamoto, M.	Small Maf proteins are obligate transcriptional cofactors for normal keratinocyte differentiation in the Keap1-Nrf2 regulatory pathway.	<i>Proc. Natl. Acad. Sci. USA</i>	101	6379-6384	2004
Morito, N., Yoh, K., Hirayama, A., Itoh, K., Nose, M., Koyama, A., Yamamoto, M. and Takahashi, S.	Nrf2 deficiency improves autoimmune nephritis caused by the <i>fas</i> mutation <i>lpr</i> .	<i>Kidney Int.</i>	65	1703-1713	2004
Ito, T., Tsukumo, S., Suzuki, N., Motohashi, H., Yamamoto, M. , Fujii-Kuriyama, Y., Mimura, J., Lin, T.-M., Peterson, R. E. Tohyama, C. and Nohara, K.	A constitutively active arylhydrocarbon receptor induces growth inhibition of Jurkat T cells through changes in the expression of genes related to apoptosis and cell cycle	<i>J. Biol. Chem.</i>	279	25204-25210	2004
Goldring, C. E. P., Kitteringham, N. R., Elsby, R., Randle, L. E., Clement, Y. N., Williams, D. P., McMahon, M., Hayes, J. D., Itoh, K., Yamamoto, M. and Park, B. K.	Activation of hepatic Nrf2 <i>in vivo</i> by acetaminophen in CD-1 Mice.	<i>Hepatology</i>	39	1267-1276	2004

Yanagawa, T., Itoh, K., Uwayama, J., Shibata, Y., Yamaguchi, A., Sano, T., Ishii, T., Yoshida, H. and Yamamoto, M.	Nrf2 deficiency causes tooth decolorization due to iron transport disorder in enamel organ.	<i>Genes Cells (Cover photo)</i>	9	641-651	2004
McMahon, M., Thomas, N., Itoh, K., Yamamoto, M. and Hayes, J.D.	Redox-regulated turnover of Nrf2 is determined by at least two separate protein domains, the redox sensitive Neh2 degron and the redox-insensitive Neh6 degron.	<i>J. Biol. Chem.</i>	279	31556-31567	2004
Cho, H-Y., Reddy, S.P.M., Yamamoto, M. and Kleeberger, S.R.	The transcription factor Nrf2 protects against pulmonary fibrosis.	<i>FASEB J.</i>	18	1258-1260	2004
Takagi, Y., Kobayashi, M., Li, L., Suzuki, T., Nishikawa, K., and Yamamoto, M.	MafT, a new member of the small Maf protein family in zebrafish.	<i>Biochem. Biophys. Res. Commun.</i>	320	62-69	2004
Kobayashi, A., Kang, M.I., Ohkawa, H., Ohtuji, M., Zenke, Y., Chiba, T., Igarashi, K. and Yamamoto, M.	Oxidative stress sensor Keap1 functions as an adaptor for Cul3-based E3 ligase to regulate proteasomal degradation of Nrf2.	<i>Mol. Cell Biol.</i>	24	7310-7319	2004
Yamamoto, T., Yoh, K., Kobayashi, K., Ishii, Y., Kure, S., Koyama, A., Sekizawa, K., Motohashi, H., and Yamamoto, M.	Methylation of polymorphisms in the promoter region of human <i>NRF2</i> gene.	<i>Biochem. Biophys. Res. Commun.</i>	321	72-79	2004
Iida, K., Itoh, K., Kumagai, Y., Oyasu, R., Hattori, K., Kawai, K., Shimazui, T., Akaza, H., and Yamamoto, M.	Nrf2 is essential for the chemopreventive efficacy of oltipraz against urinary bladder carcinogenesis.	<i>Cancer Res.</i>	64	6124-6431	2004
Rangasamy, T., Cho, C.Y., Thimmulappa, R.K., Zhen, L., Srisuma, S.S., Kensler, T.W., Yamamoto, M. , Petrache, I., Tudor, R.M., and Biswal, S.	Genetic ablation of Nrf2 enhances susceptibility to cigarette smoke-induced emphysema in mice.	<i>J. Clin. Invest.</i>	114	1248-1259	2004
McWalter, G.K., Higgins, L.G., McLellan, L.I., Henderson, C.J., Song, L., Thornalley, P.J. Itoh, K., Yamamoto, M. and Hayes, J.D.	Transcription factor Nrf2 is essential for induction of NAD(P)H:quinone oxidoreductase 1, glutathione S-transferases, and glutamate cysteine ligase by broccoli seeds and isothiocyanates.	<i>J. Nutr.</i>	134	3499S-3506S	2004
Cho, H-Y., Reddy, S.P., DeBiase, A., Yamamoto, M. and Kleeberger, S.R.	Gene expression profiling of NRF2-mediated protection against oxidative injury.	<i>Free Rad. Biol. Med.</i>	38	325-343	2005
Katsuoka, F., Motohashi, M., Engel, J.D. and Yamamoto, M.	Nrf2 transcriptionally activates the <i>mafG</i> gene through an antioxidant response element.	<i>J. Biol. Chem.</i>	280	4483-4490	2005

Katoh, Y., Iida, K., Kang, M-I., Kobayashi, A., Mizukami, M., Tong, K.I., McMahon, M., Hayes, J.D., Itoh, K. and Yamamoto, M.	Evolutionary conserved N-terminal domain of Nrf2 is essential for the Keap1-mediated degradation of the protein by proteasome.	<i>Arch. Biochem. Biophys.</i>	433	342-350	2005
Itoh, K., Tong, K.I. and Yamamoto, M.	Molecular mechanism activating Nrf2-Keap1 pathway in regulation of adaptive response to electrophiles.	<i>Free Radical Biol. Med.</i> (invited review)	36	1208-1213	2004
Motohashi, H. and Yamamoto, M.	Nrf2-Keap1 defines a physiologically important stress response mechanism.	<i>Trends Mol. Med.</i> (invited review)	10	549-557	2004
Kobayashi, M. and Yamamoto, M.	Molecular mechanisms activating Nrf2-Keap1 pathway in regulation of antioxidant genes.	<i>Antioxidants Redox Signaling</i> (invited review)	7	384-395	2005

review)

Transcription Factor Nrf2 Regulates Inflammation by Mediating the Effect of 15-Deoxy- $\Delta^{12,14}$ -Prostaglandin J₂

Ken Itoh,^{1,2†} Mie Mochizuki,^{3†} Yukio Ishii,³ Tetsuro Ishii,⁴ Takahiro Shibata,⁵ Yoshiyuki Kawamoto,⁵ Vincent Kelly,^{1,2} Kiyohisa Sekizawa,³ Koji Uchida,⁴ and Masayuki Yamamoto^{1,2*}

ERATO Environmental Response Project,¹ Institute of Basic Medical Sciences and Center for Tsukuba Advanced Research Alliance,² Institute of Clinical Medicines,³ and Institute of Social Medicines,⁴ University of Tsukuba, Tsukuba 305-8577, and Laboratory of Food and Biodynamics, Graduate School of Bioagricultural Sciences, Nagoya University, Nagoya 464-8601,⁵ Japan

Received 25 April 2003/Returned for modification 17 July 2003/Accepted 26 September 2003

Activated macrophages express high levels of Nrf2, a transcription factor that positively regulates the gene expression of antioxidant and detoxication enzymes. In this study, we examined how Nrf2 contributes to the anti-inflammatory process. As a model system of acute inflammation, we administered carrageenan to induce pleurisy and found that in Nrf2-deficient mice, tissue invasion by neutrophils persisted during inflammation and the recruitment of macrophages was delayed. Using an antibody against 15-deoxy- $\Delta^{12,14}$ -prostaglandin J₂ (15d-PGJ₂), it was observed that macrophages from pleural lavage accumulate 15d-PGJ₂. We show that in mouse peritoneal macrophages 15d-PGJ₂ can activate Nrf2 by forming adducts with Keap1, resulting in an Nrf2-dependent induction of heme oxygenase 1 and peroxiredoxin I (PrxI) gene expression. Administration of the cyclooxygenase 2 inhibitor NS-398 to mice with carrageenan-induced pleurisy caused persistence of neutrophil recruitment and, in macrophages, attenuated the 15d-PGJ₂ accumulation and PrxI expression. Administration of 15d-PGJ₂ into the pleural space of NS-398-treated wild-type mice largely counteracted both the decrease in PrxI and persistence of neutrophil recruitment. In contrast, these changes did not occur in the Nrf2-deficient mice. These results demonstrate that Nrf2 regulates the inflammation process downstream of 15d-PGJ₂ by orchestrating the recruitment of inflammatory cells and regulating the gene expression within those cells.

When animals are exposed to environmental electrophiles, including xenobiotics, drugs, toxins, and carcinogens, even at nontoxic doses, the expression of a battery of genes that are essential to cellular defense mechanisms is induced. This process of gene induction is mediated by the antioxidant-responsive element (ARE) (31, 32). An increasing number of studies have identified genes regulated by ARE. These include genes encoding the phase II detoxication enzymes, such as glutathione S-transferase and quinone reductase, as well as antioxidative defense enzymes, such as heme oxygenase 1 (HO-1) and enzymes involved in glutathione synthesis (32). The cooperative activity of these enzymes serves to detoxify electrophiles and oxidative stress products.

Nrf2 is a member of the leucine zipper transcription factor family, and its activity is pivotal for the coordinate induction of phase II detoxifying and antioxidative enzymes whose expression is under the regulatory influence of ARE (15, 16, 18, 41). Nrf2 thus contributes to cytoprotection against environmental electrophiles and oxidative stresses (1, 4, 7, 11, 16, 33). Consistent with its assigned role in protection from environmental stress, Nrf2 is highly expressed in detoxication organs, including the gastrointestinal tract, liver, kidney, and lung. In addition, Nrf2 is abundantly expressed in activated macrophages,

thyroid glands, and brown adipose tissue, suggesting additional physiological roles beyond detoxication (5).

The inflammatory response requires a coordinated integration of various signaling pathways, including cyclooxygenases (COX), nitric oxide, and cytokines (28, 40). COX enzymes catalyze the conversion of arachidonic acid to prostaglandin H₂ (PGH₂), from which other prostaglandins (PGs) are derived by the concomitant action of a variety of PG synthetases. Of the COX enzymes, COX-2 is found mainly in inflammatory cells and tissues. COX-2 is found to be upregulated during acute inflammation (37). By producing PGH₂, COX-2 promotes the synthesis of PGE₂, an important component of the inflammatory cascade that manifests many of the cardinal signs of inflammation (10). Intriguingly, since COX-2 is also expressed in the late phase of inflammation, it is widely accepted that COX-2 is associated with the resolution, as well as the establishment, of the acute inflammatory response (13). However, in contrast to the case during early stages of inflammation, pleural exudates of rats taken during the resolution stage of inflammation were found to contain high concentrations of PGD₂ and 15-deoxy- $\Delta^{12,14}$ -PGJ₂ (15d-PGJ₂) with minimal levels of PGE₂ expression.

PGs can be divided into two subtypes: conventional PGs and cyclopentenone PGs (cyPGs) (44). Conventional PGs, such as PGE₂ and PGD₂, bind to cell surface receptors to exert their actions. However, no cell surface receptors have been identified for cyPGs, such as 15d-PGJ₂ and PGA₂. Rather, cyPGs are actively transported into cells, where they accumulate in nuclei and act as potent repressors of cell growth and inducers of cell

* Corresponding author. Mailing address: Center for TARA, University of Tsukuba, 1-1-1 Tennoudai, Tsukuba 305-8577, Japan. Phone: 81-298-53-6158. Fax: 81-298-53-7318. E-mail: masi@tara.tsukuba.ac.jp.

† K.I. and M.M. contributed equally to this work.

differentiation (12, 29). It has been reported that 15d-PGJ₂ exerts its anti-inflammatory activity through activation of peroxisome proliferator-activated receptor γ (PPAR γ) (21, 34) or by directly inhibiting nuclear factor kappa B (NF- κ B) activation by binding covalently to the I κ B kinase (36).

Recently, Nrf2 target genes in macrophages were suspected of playing anti-inflammatory roles. For instance, HO-1 exerts anti-inflammatory functions in various systems, including carrageenan-induced pleurisy, through generation of carbon monoxide (30, 43). Furthermore, human peroxiredoxin I (PrxI or PAG) was recently identified as a negative regulator of macrophage migration inhibitory factor (MIF) (22), a crucial factor in the regulation of inflammation (26) and sepsis (35). These observations led us to explore possible roles for Nrf2 in the acute inflammatory response. To this end, we exploited carrageenan-induced pleurisy in mice as a model system. The results of this study reveal that the Nrf2-ARE system regulates the acute inflammation process by orchestrating the recruitment of inflammatory cells. We also found that COX-2 mediates the intracellular accumulation of 15d-PGJ₂ and that 15d-PGJ₂, which is shown to activate Nrf2, in turn regulates the expression of PrxI and other anti-oxidative stress enzymes in activated inflammatory macrophages.

MATERIALS AND METHODS

RNA blot hybridization analysis. Total cellular RNAs were extracted from macrophages by use of RNAzol (Tel-Test, Friendswood, Tex.). The RNA samples (10 μ g) were electrophoresed and transferred to Zeta-Probe GT membranes (Bio-Rad). The membranes were probed with ³²P-labeled cDNA probes as indicated in the figures. β -Actin cDNA was used as a positive control.

RT-PCR analysis. Total RNAs (1 μ g) were reverse transcribed into cDNA and used for a reverse transcription-PCR (RT-PCR) analysis (Qiagen, Hilden, Germany). GAPDH (glyceraldehyde-3-phosphate dehydrogenase) was used as a positive control. The PCR products were separated in a 1.5% agarose gel, and positive signals were quantified by densitometry analysis after staining with ethidium bromide.

Immunoblotting. The nuclei of peritoneal macrophages were solubilized with sodium dodecyl sulfate (SDS) sample buffer without loading dye and 2-mercaptoethanol, and protein concentrations were estimated by the bicinchoninic acid protein assay (Pierce, Rockford, Ill.). Proteins were separated by SDS-polyacrylamide gel electrophoresis in the presence of 2-mercaptoethanol and electrotransferred onto Immobilon membranes (Millipore). To detect immunoreactive proteins, we used horseradish peroxidase-conjugated anti-rabbit immunoglobulin G and ECL blotting reagents (Amersham). An anti-Nrf2 antibody was used as previously described (16). Inflammatory cell pellets from pulmonary lavage were lysed by sonication in buffer containing 50 mM Tris-HCl (pH 7.4), 25 mM KCl, 5 mM MgCl₂, 1 mM EDTA, 1% Nonidet P-40, and protease inhibitors. After centrifugation at 8,000 \times g for 5 min at 4°C, protein concentrations in the supernatants were determined by the Bio-Rad protein assay. Samples were boiled with gel loading buffer (62.5 mM Tris-HCl, 2% SDS, 25% glycerol, and 0.01% bromophenol blue) at a ratio of 1:1 for 5 min. Total protein equivalents for each sample were separated by SDS-5 to 15% polyacrylamide gel electrophoresis in the presence of 2-mercaptoethanol and were transferred to Sequi-Blot polyvinylidene difluoride membranes (Bio-Rad). Blots were incubated with polyclonal rabbit antibody against murine PrxI (17).

Carrageenan-induced pleurisy. Wild-type and *nrf2*^{-/-} mice of the ICR/129SV background weighing 20 to 25 g were used throughout the experiments. A 0.25% lambda carrageenan solution in saline (0.1 ml) was injected into the right pleural cavities of the animals. At 2, 6, 12, 24, 48, and 72 h and 7 days after the injection of carrageenan, the chest was carefully opened and the pleural cavity was washed with 1 ml of saline solution containing heparin. The pleural cavity was washed five times consecutively in the same way, and the pleural lavage fluid was collected into a tube.

Leukocyte counts. A 30- μ l sample of collected pleural lavage fluid was diluted with Turk's solution, and total leukocytes were counted under an optical microscope. Differential leukocyte counts were determined in cytospin smears stained with Wright-Giemsa stain (Diff-Quick; Sysmex, Kobe, Japan).

TABLE 1. Number of neutrophils and albumin concentration in pleural lavage fluid

Time (h) and treatment	Neutrophils (10 ⁴) ^a		Albumin (mg/ml) ^a	
	Nrf2 ^{+/+} mice	Nrf2 ^{-/-} mice	Nrf2 ^{+/+} mice	Nrf2 ^{-/-} mice
0	1 \pm 0	1 \pm 0	0.27 \pm 0.07	0.30 \pm 0.14
12				
Vehicle	179 \pm 53 ^c	128 \pm 48	0.38 \pm 0.14	0.26 \pm 0.09
Carrageenan	492 \pm 59 ^{b,c}	508 \pm 56 ^{b,c}	0.68 \pm 0.22 ^{b,c}	0.87 \pm 0.36 ^{b,c}
24				
Vehicle	27 \pm 18	21 \pm 14	0.30 \pm 0.18	0.31 \pm 0.22
Carrageenan	229 \pm 10 ^{b,c}	386 \pm 56 ^{b,c}	1.1 \pm 0.30 ^{b,c}	1.5 \pm 0.26 ^{b,c}

^a Data are means \pm SEM. At least three mice were examined for each group.

^b Significantly different from time-matched vehicle control mice ($P < 0.05$).

^c Significantly different from genotype-matched 0-h control mice ($P < 0.05$).

Albumin concentration. The first washing was centrifuged at 400 \times g for 5 min at 4°C, and the albumin concentration in the supernatant was determined with the albumin reagent from Sigma (St. Louis, Mo.).

Immunohistochemical analysis. Cells were smeared onto poly-L-lysine-coated slides and allowed to air dry. Endogenous peroxidases were quenched with 0.3% H₂O₂ in methanol, and sections were washed with 0.1% Triton X-100 in phosphate-buffered saline. The sections were reacted with anti-15d-PGJ₂ monoclonal antibody (38), anti-PrxI antibody (16), anti-HO-1 antibody (a generous gift from Shigeru Taketani), anti-F4/80 antibody (Serotec), anti-COX-2 antibody (Santa Cruz), or anti-hematopoietic PG synthetase (PGDS) antibody (Santa Cruz) and incubated for another hour with Histofine Simple Stain MAX-PO (Nichirei, Tokyo, Japan). Diaminobenzidine was used as a chromogen.

NS-398 and indomethacin treatment. NS-398 (Cayman Chemical, Ann Arbor, Mich.) (10 mg/kg) and indomethacin (Sigma) (10 mg/kg) were administered intraperitoneally 1 h before the injection of carrageenan. The pleural cavity was washed at 2, 12, and 24 h after the injection of carrageenan for the determination of inflammatory cell numbers and albumin concentration. To determine the effects of NS-398 at 48 and 72 h and 7 day, NS-398 was administered every 24 h thereafter. At 48 h, 72 h, and 7 days after the injection of carrageenan, the pleural cavity was washed for the determination of inflammatory cell numbers and albumin concentration.

15d-PGJ₂ administration. At 1 h after the intraperitoneal injection of NS-398, 15d-PGJ₂ (100 μ g/kg) was injected into the pleural cavity. At 24 h after the injection of carrageenan, the pleural cavity was washed for the determination of inflammatory cell numbers and anti-inflammatory gene expression levels.

Statistical analysis. Statistical analysis was done by analysis of variance followed by a Bonferroni posttest. Albumin concentration data were analyzed by using Welch's *t* test. A *P* value of less than 0.05 was accepted as statistically significant.

RESULTS

Persistence of inflammatory cells in *nrf2*^{-/-} mice during carrageenan-induced pleurisy. To explore the influence of Nrf2 during acute inflammation, we examined the effect of *nrf2* gene disruption on carrageenan-induced pleurisy in mice. In our preliminary experiments we administered 1% carrageenan to mice, a dose that is commonly used to induce carrageenan pleurisy in rodents, but we found that this particular dose provoked severe and protracted inflammation in mice as judged by neutrophil infiltration into the pleural cavity. We therefore carefully tested the correlation between the carrageenan dose and the duration of inflammation, finding that administration of 0.25% carrageenan reproduces the time course of acute inflammation and recovery (data not shown). Vehicle treatment caused a transient infiltration of neutrophils, which peaked at 12 h, but did not significantly alter the

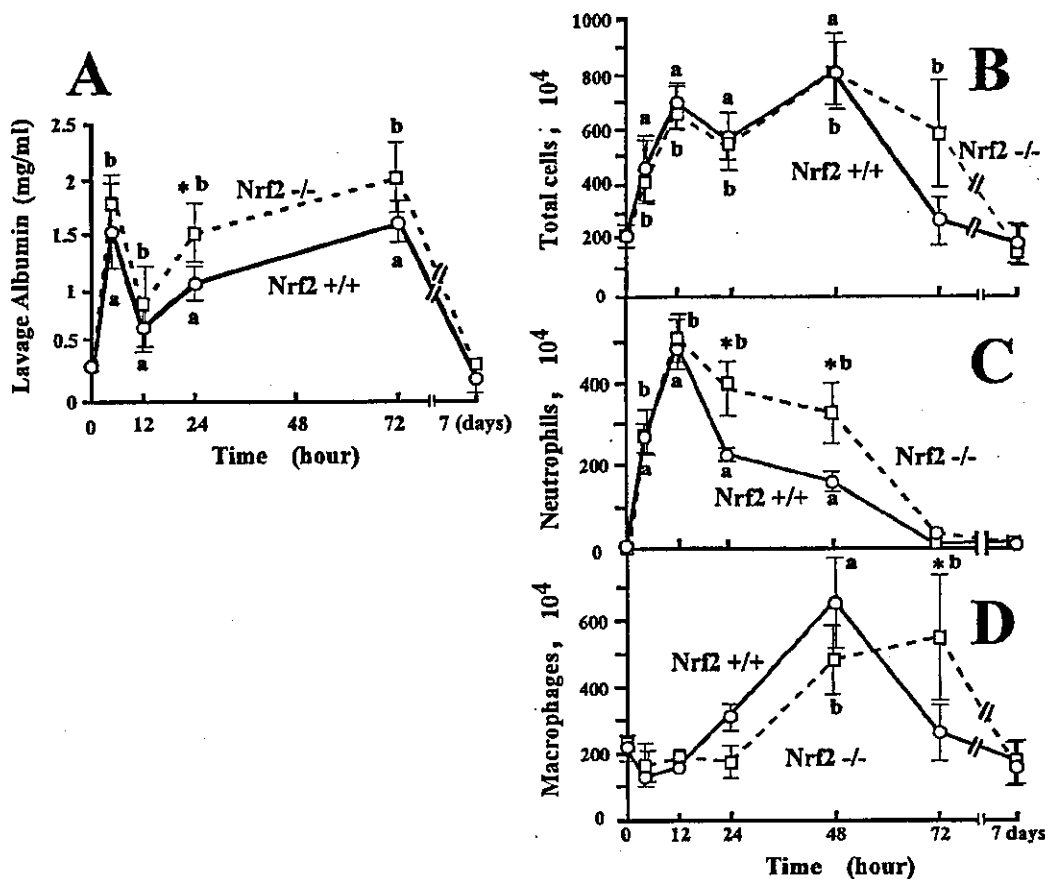


FIG. 1. Persistence of inflammatory cells in *Nrf2*-deficient mice in carrageenan-induced pleurisy. (A) Concentrations of pleural lavage albumin were measured at the indicated time points of pleurisy, and the means and standard deviations of triplicates are shown. (B to D) The numbers of total inflammatory cells (B), neutrophils (C), and macrophages (D) were counted microscopically at the indicated time points of pleurisy, and the means and standard deviations of triplicates are shown. Solid lines indicate the results for *nrf2*^{+/+} mice, whereas dashed lines indicate the results for *nrf2*^{-/-} mice. The means from four experiments are presented with standard errors of the mean. *, significantly different from time-matched wild-type mice ($P < 0.05$). a, significantly different from non-carrageenan-treated wild-type mice at the 0-h time point ($P < 0.05$). b, significantly different from non-carrageenan-treated *nrf2*^{-/-} mice at the 0-h time point ($P < 0.05$).

albumin concentration (Table 1) and macrophage recruitment (data not shown) at the 12- and 24-h time points. In contrast, 0.25% carrageenan provoked a significant increase of neutrophil and albumin concentrations in the pleural lavage fluid (Table 1) compared to the vehicle-treated mice.

The albumin concentration in the pleural lavage fluid showed two peaks, one at 2 h and the other at 72 h after carrageenan injection, and then returned to normal levels by day 7 of pleurisy in both wild-type and *nrf2*^{-/-} mice (Fig. 1A). The albumin concentration in pleural lavage fluid was significantly higher in *nrf2*^{-/-} mice during pleurisy than in wild-type mice at the 24-h time point. The total inflammatory cell number in the pleural lavage fluid peaked at 12 and 48 h of pleurisy in both wild-type and *nrf2*^{-/-} mice (Fig. 1B), but the infiltration of the cells persisted until 72 h of pleurisy in *nrf2*^{-/-} mice. We speculated that an increase in neutrophils and macrophages at different time points might be responsible for the two peaks of infiltrated cells. We therefore examined the numbers of neutrophils (Fig. 1C) and macrophages (Fig. 1D) in the pleural lavage fluid. In wild-type mice, the neutrophil number

peaked at 12 h and returned to the background level at 72 h of pleurisy, indicating that the first peak of total infiltrated cells mainly reflected an increase in neutrophils. Although in *nrf2*^{-/-} mice, the magnitude of neutrophil infiltration was not significantly different from that in wild-type mice, the increased number of neutrophils persisted to later time points of pleurisy. The number of neutrophils in the pleural lavage fluid from *nrf2*^{-/-} mice was significantly higher than that in wild-type mice at 24 and 48 h (Fig. 1C).

In contrast, macrophages were recruited to the pleural space at a later phase of pleurisy than the peak of neutrophil infiltration (Fig. 1D). The increase of macrophage number peaked at 48 h after the carrageenan administration and returned to the control level at the 72-h time point in wild-type mice, indicating that the second peak of total infiltrated cells mainly reflected an increase in macrophages. In contrast, macrophage recruitment peaked at the 72-h time point in *nrf2*^{-/-} mice. The number of macrophages at this time point was significantly different from that in wild-type mice (Fig. 1D). Collectively, these results demonstrate that *Nrf2* deficiency leads to a per-

sistence of neutrophil occupation and a delay of macrophage recruitment in carrageenan-induced pleurisy of mice.

15d-PGJ₂ accumulates in pleural inflammatory macrophages. Since 15d-PGJ₂ has been implicated as a key regulator of carrageenan pleurisy (8, 13, 44), we examined whether 15d-PGJ₂ accumulates in pleural inflammatory cells by using a specific monoclonal antibody against 15d-PGJ₂. The antibody has successfully detected the accumulation of 15d-PGJ₂ in both RAW264.7 cells activated by lipopolysaccharide and foamy macrophages of human atherosclerotic lesions (38). Furthermore, this antibody has shown to react almost exclusively with 15d-PGJ₂ (38). Immunohistochemical analysis with this antibody revealed that accumulation of 15d-PGJ₂ specifically occurred in pleural macrophages that were positive for F4/80 antigens but did not occur in neutrophils (data not shown).

As reported previously for rat carrageenan pleurisy, the accumulation of 15d-PGJ₂ showed two peaks (13). The accumulation of 15d-PGJ₂ was transiently observed at 2 h of pleurisy (Fig. 2A), but the accumulation then decreased at 6 h of pleurisy (Fig. 2B). At 2 h of pleurisy, the inducible accumulation of 15d-PGJ₂ in macrophages appeared to occur strongly around the nuclear membranes of resident pleural macrophages, which are small and round. The level increased again at 12 h after the carrageenan injection and remained high until 48 h of pleurisy (Fig. 2C and data not shown), followed by another increase at 72 h of pleurisy (Fig. 2D). At the 24-h time point, the accumulation of 15d-PGJ₂ was observed mainly in the cytoplasm of macrophages, which were large and had a foamy appearance (Fig. 2C). These results thus demonstrate that 15d-PGJ₂ specifically accumulates in pleural inflammatory macrophages and suggest that 15d-PGJ₂ may act through modifying macrophage function.

The Nrf2-Keap1 pathway mediates the induction of a range of genes by 15d-PGJ₂ in mouse peritoneal macrophages. cyPGs, including 15d-PGJ₂, have a reactive α,β -unsaturated carbonyl group in the cyclopentane ring. This ring structure renders this molecule capable of forming Michael adducts with nucleophilic cellular molecules and covalent modification of specific proteins. We speculate that this feature of cyPGs may activate Nrf2 (39). In order to obtain solid evidence for activation of the Nrf2 pathway by 15d-PGJ₂, we first examined the effect of exogenous 15d-PGJ₂ on the induction of three Nrf2 target genes in primary cultures of mouse peritoneal macrophages, which were used previously for the study of Nrf2 (16). The results clearly indicated that 15d-PGJ₂ activates, in a dose-dependent manner, the expression of the *HO-1*, *Prx1*, and *A170* genes (Fig. 3A), all of which were shown to be inducible by electrophiles in peritoneal macrophages (16).

We then examined which prostaglandins could strongly activate Nrf2 by using the peritoneal macrophage system. Of arachidonic acid and the arachidonic acid metabolites, including PGA₁, PGB₂, PGD₂, PGE₂, PGF_{1 α} , 15d-PGJ₂, thromboxane B₂, and leukotriene B₄, only PGA₁, 15d-PGJ₂, and PGD₂ markedly induced the expression of Nrf2 target genes (Fig. 3B). PGA₁ and 15d-PGJ₂ are classified as electrophilic cyPGs. Since PGD₂ is readily metabolized to 15d-PGJ₂ (38), 15d-PGJ₂ is suggested to be the most important cyPG in the regulation of Nrf2.

cyPGs activate Nrf2 in macrophages and hepatocytes. Subsequently, we examined the requirement for Nrf2 in the induc-

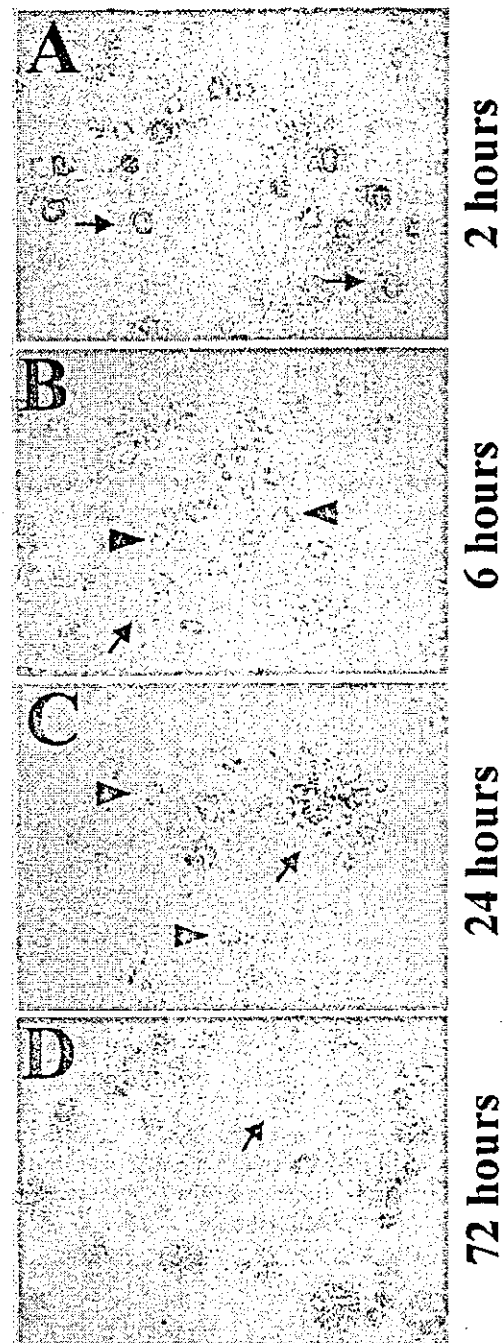


FIG. 2. Accumulation of 15d-PGJ₂ (brown) in pleural macrophages during carrageenan-induced pleurisy. Pleural inflammatory cells were examined immunohistochemically at the indicated times of pleurisy with anti-15d-PGJ₂ antibody. Arrows indicate macrophages, while arrowheads indicate neutrophils.

tion of antioxidant genes, using primary cultures of peritoneal macrophages from Nrf2-deficient mice. While *HO-1*, *Prx1*, and *A170* mRNAs were all induced in wild-type macrophages by the addition of 5- μ M 15d-PGJ₂ to the culture medium (Fig. 4A, lane 2), the induction was not observed in *nrf2*^{-/-} macro-

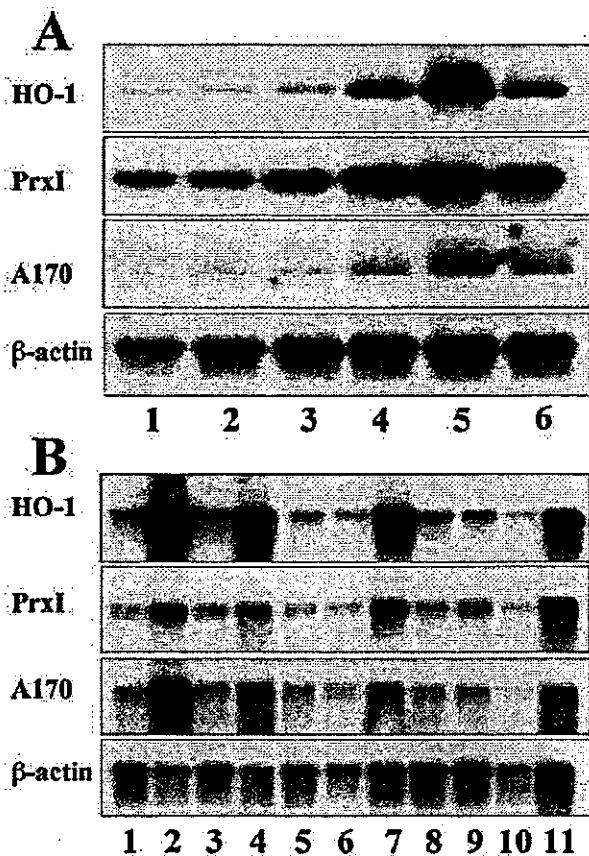


FIG. 3. cyPGs activate a set of antioxidant and anti-inflammatory genes in mouse peritoneal macrophages. (A) Peritoneal macrophages were treated with dimethyl sulfoxide alone (lane 1); with 15d-PGJ₂ at 0.5 μM (lane 2), 1 μM (lane 3), 5 μM (lane 4), or 10 μM (lane 5) for 5 h; or with 100 μM diethylmaleate for 5 h (lane 6), and total RNAs were analyzed by RNA blot analysis with HO-1, PrxI, and A170 cDNAs as probes. A β-actin cDNA probe was used for a loading control. (B) Peritoneal macrophages were treated with dimethyl sulfoxide alone (lane 1), PGA₁ (50 μM) (lane 2), PGB₂ (50 μM) (lane 3), PGD₂ (50 μM) (lane 4), PGE₂ (50 μM) (lane 5), PGF_{1α} (50 μM) (lane 6), 15d-PGJ₂ (10 μM) (lane 7), thromboxane B₂ (50 μM) (lane 8), leukotriene B₄ (1 μM) (lane 9), arachidonic acid (50 μM) (lane 10), or diethylmaleate (100 μM) (lane 11). Total RNA fractions were analyzed by RNA blot analysis as for panel A.

phages (lane 6). The result was reproducible with 10-μM 15d-PGJ₂ (lanes 3 and 7), but in this case a weak induction was observed in the *nrf2*^{-/-} macrophages (lane 7), suggesting the presence of a minor complementary pathway to Nrf2. Consistent with these results, immunoblot analysis with anti-Nrf2 antibody revealed that 15d-PGJ₂ (Fig. 4B, lane 3) and PGA₁ (lane 4), but not PGE₂ (lane 5), induced the nuclear accumulation of Nrf2.

Immunocytochemical analysis of the rat hepatocyte cell line RL34, using the anti-Nrf2 antibody, further demonstrated that under normal culture conditions Nrf2 is retained by Keap1 in the cytoplasm (Fig. 4C). However, after the addition of 15d-PGJ₂, Nrf2 is liberated from Keap1 and translocates to and accumulates within the nucleus (Fig. 4D).

Recent studies indicate that certain Nrf2 inducers, such as

Michael reaction acceptors, directly bind to reactive cysteine residues in Keap1, thereby liberating Nrf2 (9). To elucidate whether 15d-PGJ₂ binds directly to Keap1, we examined the binding of biotin-tagged 15d-PGJ₂ to Keap1 in RL34 cells. A pull-down analysis with avidin beads followed by probing with anti-Keap1 antibody demonstrated that Keap1 could be detected in precipitates from biotinylated 15d-PGJ₂-treated or biotinylated Δ¹²-PGJ₂-treated cells but not in the control immunoprecipitates (Fig. 4E). This result suggests that 15d-PGJ₂ directly binds to Keap1, most probably through covalent linkage, allowing Nrf2 to be released from Keap1.

COX-2 inhibitor affects the inflammatory cell infiltration. In order to elucidate the relationship between the accumulation of 15d-PGJ₂ and activation of Nrf2, we examined the time course of PrxI gene expression during the carrageenan-induced pleurisy. Immunoblot analyses with anti-PrxI antibody revealed that the expression of PrxI was induced at as early as 2 h of pleurisy (Fig. 5A, lanes 3 to 5). In contrast, the induction of PrxI during pleurisy was largely abolished in *nrf2*^{-/-} mice, and this difference was prominent at 2 to 24 h (lanes 4, 7, and 10) but became relatively small after 48 h of pleurisy (lanes 13 and 16).

COX-2 is known to regulate PG synthesis in carrageenan pleurisy. To examine the role of COX-2 in the inducible expression of PrxI, we examined the *in vivo* effect of NS-398, a specific inhibitor of COX-2 (42), on PrxI expression. Peritoneal injection of NS-398 1 h before carrageenan treatment significantly attenuated the expression of PrxI in macrophages when tested by immunoblotting (Fig. 5A) and of 15d-PGJ₂ when tested by immunocytochemistry (data not shown). NS-398 caused a reduction of PrxI expression especially at 2 to 24 h (Fig. 5A, lanes 5, 8, and 11), but the effect was not as prominent after 48 h of pleurisy (lanes 14 and 17). These results suggest a possible scenario in which COX-2 mediates the accumulation of 15d-PGJ₂ and 15d-PGJ₂ in turn activates Nrf2 and regulates the expression of PrxI as well as the other antioxidant genes.

Immunohistochemical analysis demonstrated that PrxI expression was specifically observed in macrophages, but not in neutrophils, of pleural lavage fluid (Fig. 5B). The expression profile of PrxI clearly overlapped with those of 15d-PGJ₂ and macrophage-specific F4/80 antigen (Fig. 5B). The expression of HO-1 was also detected exclusively in pleural macrophages (Fig. 5B), in very good agreement with previous analysis of the rat pleurisy model. Furthermore, COX-2 and hematopoietic PGDS, two major rate-limiting enzymes for 15d-PGJ₂ synthesis, were highly expressed in the macrophages (Fig. 5B), supporting our contention that 15d-PGJ₂ was synthesized mainly in the macrophages.

It should be noted that NS-398 treatment caused a persistence of neutrophil infiltration at 24 h of pleurisy (Fig. 5C) and a delay in macrophage recruitment (Fig. 5D) in pleural lavage fluid. This is in contrast to the case for untreated mice, where the macrophage number was high at 48 h and decreased at 72 h of pleurisy. It can be observed that in the NS-398-treated mice the macrophage number continued to climb even at 72 h of pleurisy (Fig. 5D). Also, in the NS-398-treated mice, the macrophage number was rather low at the 24- and 48-h time points, indicating a delay in macrophage recruitment. The persistence of neutrophil infiltration and the delay of macrophage

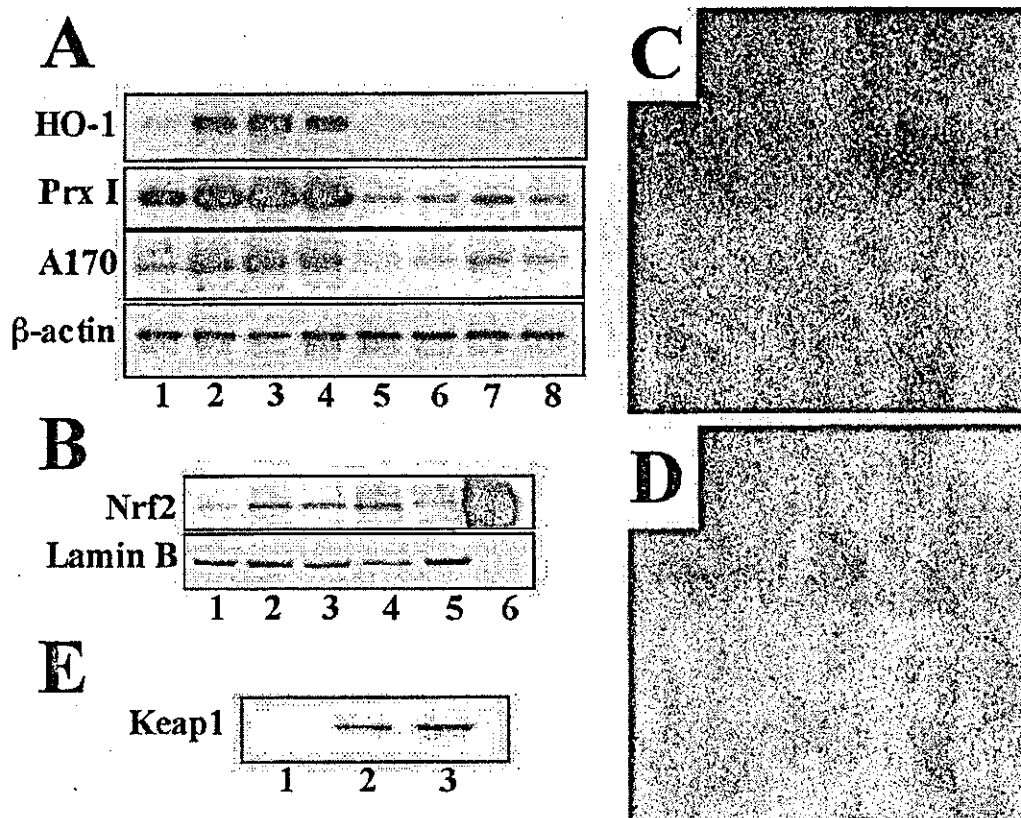


FIG. 4. cyPGs activate Nrf2 in macrophages and hepatocytes. (A) Peritoneal macrophages derived from either wild-type mice (lanes 1 to 4) or *nrf2*^{-/-} mice (lanes 5 to 8) were treated with 5 μ M (lanes 2 and 6) or 10 μ M (lanes 3 and 7) 15d-PGJ₂ or with 100 μ M diethylmaleate (lanes 4 and 8). Untreated controls are shown in lanes 1 and 5. Total RNAs were analyzed by RNA blotting analysis, using cDNAs for HO-1, PrxI, or A170 as probes. A β -actin cDNA probe was used for a loading control. (B) Nuclear extracts were prepared from macrophages untreated (lane 1) or treated with diethylmaleate (100 μ M) (lane 2), 15d-PGJ₂ (5 μ M) (lane 3), PGA₁ (100 μ M) (lane 4), or PGE₂ (100 μ M) (lane 5). The extracts were immunoblotted with anti-Nrf2 antibody or anti-lamin B antibody. Recombinant Nrf2 in 293T cells was also loaded as a control (lane 6). (C and D) RL34 cells were either untreated (C) or treated with 10 μ M 15d-PGJ₂ for 4 h (D), and expression of Nrf2 were examined immunocytochemically with the anti-Nrf2 antibody. Subcellular localization of Nrf2 was analyzed by confocal microscopy. (E) RL34 cells were treated with dimethyl sulfoxide (lane 1), biotinylated Δ^{12} -PGJ₂ (lane 2), or biotinylated 15d-PGJ₂ (lane 3). Keap1-PGJ₂ complexes were precipitated from the cell extracts with avidin beads and probed with the anti-Keap1 antibody.

recruitment were also observed in the COX-1/COX-2 dual inhibitor indomethacin (Fig. 5E). Thus, inflammatory cell infiltration in COX-2-inhibited mice closely reflects that observed in Nrf2-deficient mice, further supporting our contention that 15d-PGJ₂ (and COX-2) acts as a regulator of the Nrf2 pathway and the expression of antioxidant genes.

Replacement of 15d-PGJ₂ into the intrapleural space. Finally, we wished to test directly the significance of 15d-PGJ₂ accumulation in the development of and recovery from carrageenan-induced pleurisy. To this end, we administered 15d-PGJ₂ into the intrapleural cavity and examined changes in inflammatory cell infiltration at 24 h of pleurisy. Consistent with the results shown above, administration of NS-398 to mice with pleurisy increased the neutrophil number at 24 h (Fig. 6A, bar 2). We found that simultaneous injection of 15d-PGJ₂ with carrageenan into the pleural space reversed the increase of neutrophil infiltration in NS-398-treated mice (bar 3). The important finding here is that the administration of 15d-PGJ₂ into the pleural space of Nrf2-null mice did not affect the accumulation of neutrophils (compare bars 4 and 5).

We found the opposite result for macrophages recruitment during pleurisy. While the NS-398 treatment provoked a delay in the macrophage recruitment (Fig. 6B, bar 2), this was reversed by the simultaneous administration of 15d-PGJ₂ (bar 3). Nrf2 must therefore mediate this effect of 15d-PGJ₂, as 15d-PGJ₂ did not help to reverse the delay in macrophage recruitment in the Nrf2-deficient mice (compare bars 4 and 5).

To determine changes in the antioxidant gene expression, we carried out RT-PCR analyses with pleural inflammatory cells and specific primers for PrxI (Fig. 6C) and HO-1 (Fig. 6D). The expression of PrxI and HO-1 showed a pattern of changes similar to that for macrophage number. The NS-398-treatment produced a decrease in *PrxI* and *HO-1* gene expression (bar 2). On the other hand, the administration of 15d-PGJ₂ to the NS-398-treated mice reversed the PrxI and HO-1 mRNA expression level (bar 3) to that for wild-type control mice (bar 1). The expression levels of PrxI and HO-1 mRNAs in the Nrf2-deficient mice did not change with 15d-PGJ₂ treatment (compare bars 4 and 5). These results thus argue that 15d-PGJ₂ transduces the inflammatory signals to Nrf2 and that Nrf2

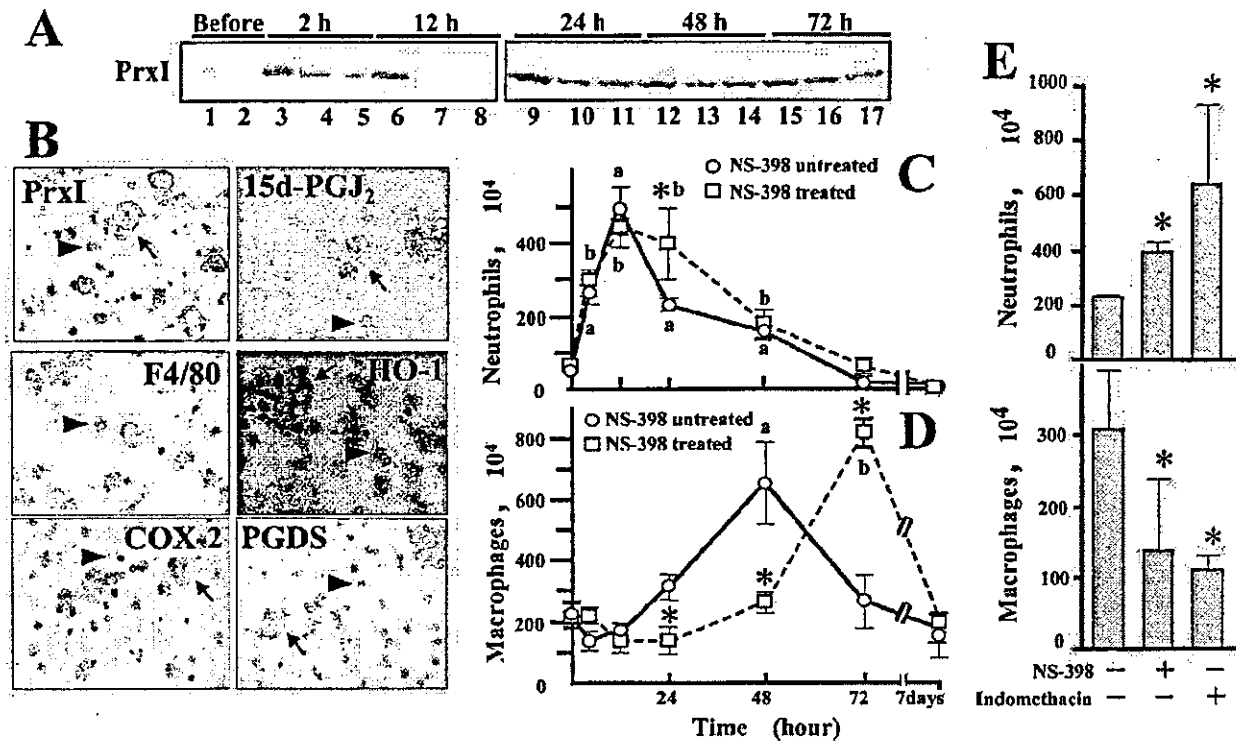


FIG. 5. PrxI expression at the early phase of carrageenan-induced pleurisy depends on both 15d-PGJ₂ and Nrf2. (A) Both the COX-2 inhibitor NS-398 and *nrf2* gene disruption affect PrxI expression during carrageenan-induced pleurisy. Whole-cell extracts of pleural inflammatory cells from wild-type mice (lanes 1, 3, 6, 9, 12, and 15), *nrf2*^{-/-} mice (lanes 2, 4, 7, 10, 13, and 16), or NS-398-treated wild-type mice (lanes 5, 8, 11, 14, and 17) at the indicated time points of pleurisy were examined by immunoblotting with anti-PrxI antibody. (B) The expression of PrxI, 15d-PGJ₂, F4/80, HO-1, COX-2, and hematopoietic PGDS in pleural inflammatory cells at 24 h of pleurisy was analyzed immunohistochemically with the corresponding antibodies as indicated. Arrows indicate macrophages, while arrowheads represent neutrophils. (C and D) Administration of NS-398 affects neutrophil (C) and macrophage (D) numbers during carrageenan-induced pleurisy. The number of pleural inflammatory cells was microscopically counted, and the means from four experiments are presented with standard errors of the mean. *, significantly different from time-matched NS398-untreated mice ($P < 0.05$). a, significantly different from carrageenan-untreated wild-type mice at the 0-h time point ($P < 0.05$). b, significantly different from carrageenan-untreated *nrf2*^{-/-} mice at the 0-h time point ($P < 0.05$). (E) Effect of indomethacin on pleural inflammatory cells. Cell counts were taken at 24 h of pleurisy. The means from four experiments are presented with standard errors of the mean. *, significantly different from untreated control mice ($P < 0.05$).

transcriptionally regulates both the antioxidant gene expression in pleural macrophages and inflammatory cell recruitment.

DISCUSSION

The cyPG 15d-PGJ₂ is emerging as a probable regulator of acute inflammation (13, 43–45). By exploiting carrageenan-induced pleurisy as a model system for acute inflammation, this study examined the relationship between 15d-PGJ₂ and Nrf2. We found that during carrageenan-induced pleurisy, 15d-PGJ₂ accumulates in pleural inflammatory cells and the accumulation is confined to macrophages. The results of this study unveil a number of significant correlations between accumulation of 15d-PGJ₂ and activation of Nrf2 during carrageenan-induced pleurisy. First, in *Nrf2*-deficient mutant mice, the accumulation of neutrophils during inflammation persisted and macrophage recruitment was delayed to the late phases of pleurisy. Second, the COX-2 inhibitor NS-398 and the COX-1/COX-2 dual inhibitor indomethacin, which attenuate the accumulation of 15d-PGJ₂, affected the acute inflammatory response in a manner similar to a deficiency in Nrf2. NS-398

repressed the expression of PrxI in pleural macrophages and caused a persistence of neutrophil accumulation with a concomitant delay in macrophage recruitment. Third, the administration of 15d-PGJ₂ into the pleural space reversed both the decrease of PrxI expression and persistence of neutrophils in NS-398-treated mice, whereas this treatment did not reverse a similar phenotype in the *Nrf2*-deficient mice, arguing strongly that 15d-PGJ₂ functions to activate Nrf2. Fourth, our data show that in peritoneal macrophages and hepatocytes, 15d-PGJ₂ directly bound to Keap1 and thereby liberated Nrf2. Taken together, these results demonstrate that Nrf2 regulates the acute inflammatory response by orchestrating the recruitment of inflammatory cells and regulating the expression of anti-oxidative stress genes downstream of 15d-PGJ₂.

Increasing lines of evidence (8, 44, 45) suggest that in addition to establishing acute inflammation, COX-2 also contributes to the resolution phase of inflammation through 15d-PGJ₂. 15d-PGJ₂ can function as both an activator and a repressor of signal-transducing transcription factors. The possible contributions made by 15d-PGJ₂ to the acute inflammatory response are summarized in Fig. 7. It has been reported